An accurate and efficient eikonal equation solver with variable grid spacing

Wen-Jing Wu, Geo-X Systems Ltd., Calgary

2004 CSEG National Convention

Introduction

The eikonal equation solver is widely used in seismology. Although many authors have discussed various numerical methods for solving the eikonal equation (e. g. Vidale, 1988, 1990; Podvin and Lecomte, 1991; and Hole and Zelt, 1995), the topic still warrants further treatment. In this paper I will first analyze the errors inherent in the finite difference schemes, then illustrate them via numerical examples. Next I will present a new implementation, which employs variable grid spacing to solve the eikonal equation accurately and efficiently.

The finite-difference scheme of the eikonal equation

For simplicity I consider 2-D here, and it is easy to extend to 3-D. The eikonal equation can be written as

$$\left(\partial T/\partial x\right)^2 + \left(\partial T/\partial z\right)^2 = 1/v^2 \quad , \tag{1}$$

where T is traveltime and v is velocity. It is not difficult to derive a numerical formula for a finite-difference scheme in case of a rectangular grid (i. e. $\Delta x \neq \Delta z$). The basic formula can be written as

$$T_4 = (-B \pm \sqrt{B^2 - 4AC})/(2A) \tag{2}$$

with $A = 1/(\Delta x)^2 + 1/(\Delta z)^2$, $B = 2\left[(T_2 - T_1 - T_3)/(\Delta x)^2 + (T_3 - T_1 - T_2)/(\Delta z)^2\right]$, and $C = (T_2 - T_1 - T_3)^2/(\Delta x)^2 + (T_3 - T_1 - T_2)^2/(\Delta z)^2 - 4/v^2$,

where T_1, T_2, T_3 and T_4 are traveltimes, $\Delta x, \Delta z$ are grid spacings in the x and z directions respectively (see Fig. 1). If $\Delta x = \Delta z = h$, we have

$$T_4 = T_1 \pm \sqrt{2h^2/v^2 - (T_2 - T_3)^2} \quad , \tag{3}$$

which is the basic extrapolation formula of Vidale (1988). Vidale points out that this equation is perfect only for a plane wave with constant velocity. Here we show it. For simplicity again we consider Eq. (3) (i. e. $\Delta x = \Delta z = h$). In Fig, 1, we have

$$T_4 = T_1 + \overline{AE}/v \text{, and } \overline{AE} = \sqrt{2h^2 - (\overline{DE})^2} \tag{4}$$

It is easy to prove that

$$\overline{DE} = \overline{CF} = v\left|T_2 - T_3\right| \tag{5}$$

Substituting (5) into (4), we obtain Eq. (3).

Obviously, Eq. (3) is not exact if there is not a plane wave and/or a constant velocity.

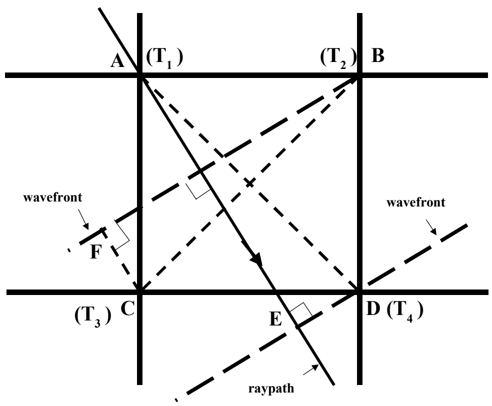

Figure 1

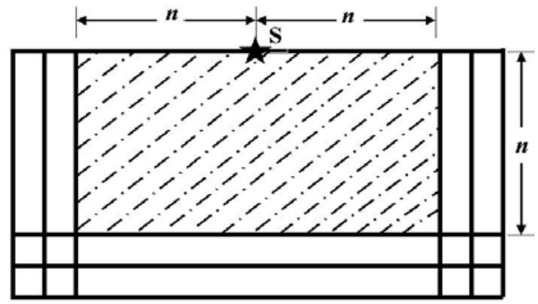

Figure 2

Error analysis

We will analyze the errors when (a) the wave is no longer a plane wave; and (b) the velocity is not constant.

(1) A constant velocity model

First, we consider a constant velocity model and a point source. It is well known that the wave is far from a plane wave at the area near the source and it is approximately a plane wave at the area with the larger distance from the source. I put the accurate traveltimes at the dashed rectangular area with the number of grid points n from the source, and I calculate the traveltimes of the next two grid points from the dashed area on each of the 3 sides as shown in Fig. 2. The absolute errors (traveltime is in units of one grid spacing: h/v) are decrease with the number n as expected (Fig. 3).

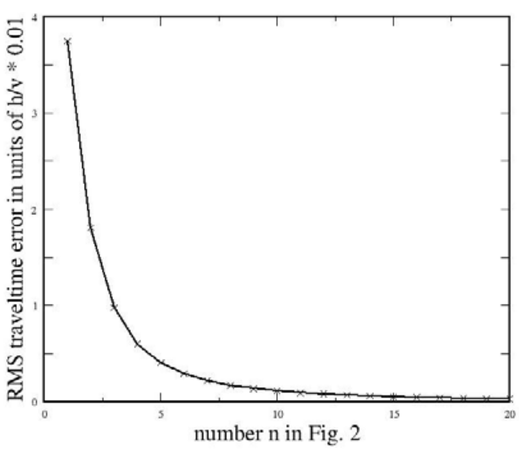

Fig. 3. RMS absolute errors in traveltime of one grid spacing (%) decrease when the wave is closer to a plane wave.

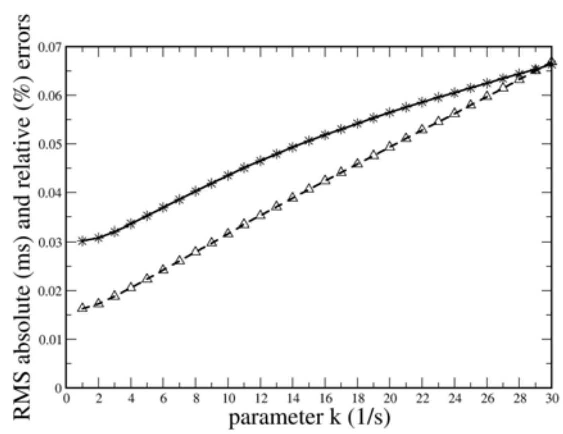

Fig. 4. RMS absolute errors (ms, solid line with stars) and RMS relative errors (%, dashed line with triangles) increase with the parameter k.

(2) The velocity linearly increases with depth z: $V = V_0 + kz$.

In this case an analytical formulae can be used to calculate accurate traveltimes (e. g. Telford, et al., 1976). The traveltimes (t) are determined by

$$\left(\frac{V_0}{k}\right)^2 \sinh^2 kt - x^2 - \left[z - \frac{V_0}{k}\left(\cosh kt - 1\right)\right]^2 = 0 , \qquad (6)$$

where z is the depth, and x is the horizontal distance from the source. The value of the k determines how far the velocity departs from a constant velocity. Consider a model similar to Fig. 2. Again I set the accurate traveltimes in the dashed area, and calculate the traveltimes from n+1 to 2n. Here I choose n=10 to reduce the errors caused by "non-plane wave" effect described above (thereby isolating the "variable velocity" effect presently studied), and set v0=1000m/s, h=10m. I calculate the errors for k=1 s^{-1} to 30 s^{-1}. The results are shown in Fig,. 4. Both the RMS absolute (ms) and relative (%) errors are increasing with k.

The variable grid spacing method

The analysis shows that the errors in the eikonal equation solver come from the both the non-plane wave and the variable velocity effects. Obviously both these errors would be reduced when a small grid spacing is used. To show this I consider the linearly increased velocity model mentioned above. The calculation area is 200 m deep and 400 m wide, and the source is set at the middle point of the surface. The velocity increases linearly from 2000 m/s at the surface to 8000 m/s at the bottom (i. e. $k = 30s^{-1}$). I choose the initial value of grid spacing h=20m, then apply smaller grid spacing h/l, l=1 to 10 to reduce errors. The results are shown in Fig. 5(a) and (b). Both absolute and relative RMS errors decrease when l increases; i. e. the grid spacing decreases. The RMS absolute errors almost linearly increase with the grid spacing. In practice, velocity models often contain quite large velocity contrasts. If the velocity changes from 2500 m/s to 6500 m/s within a few grid spacings, over 40 m for example, the equivalent local k would be 1000 s^{-1}. The small grid spacing may be necessary to avoid larger errors. Using small grid spacing can reduce errors in travel times, but it dramatically increases computation cost especially for 3-D models. Fortunately, there is typically only a small portion of the seismic velocity model with the large velocity contrast, Thus the variable grid spacing method can be used to solve the eikonal equation accurately and efficiently. The small grid spacing is only used for the areas with the larger velocity contrasts, and generally the grid spacing can vary according to the local velocity contrast. Although in principle the small grid spacing could also used for improved accuracy in the near-source zone where the wavefronts are non-planar, in practice it is only necessary to use a near-source small grid in those cases where the near-source velocity field varies rapidly. In cases where the near-source velocities vary slowly, errors due to the near-source curved wavefront effect can easily be handled by direct computation of source traveltimes via analytic expressions based on a best fit constant velocity or constant gradient model (e. g., Aldridge and Oldenburg, 1993).

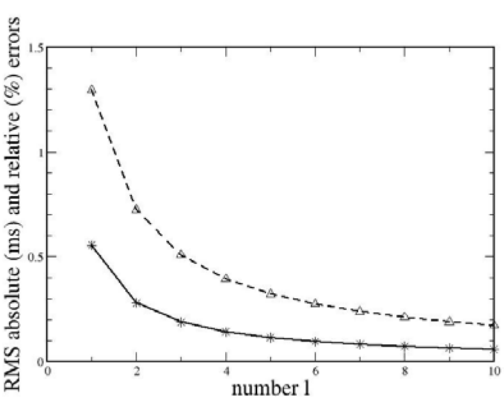

Fig. 5(a) RMS absolute error (ms, solid line with stars) and RMS relative errors (%, dashed line with triangles) decrease when the number l increases.

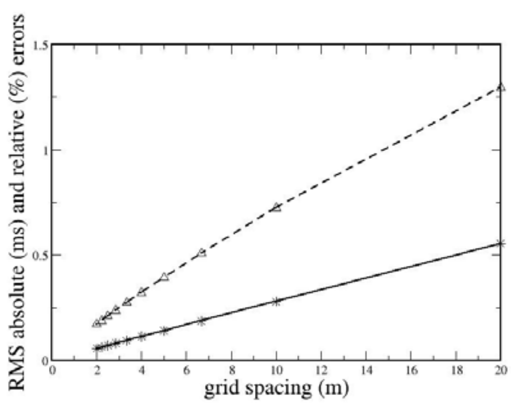

Fig. 5(b) RMS absolute error (ms, solid line with stars) and RMS relative errors (%, dashed line with triangles) increase with the grid spacing.

This variable grid spacing method in the eikonal equation solver has many applications in seismic processing. An efficient and robust eikonal equation solver is crucial for Kirchhoff depth migration. It is even useful for Kirchhoff time migration, because the traveltimes calculated by the eikonal equation can be more accurate than those obtained by the Dix equation. Moreover, using the eikonal equation to calculate first arrival traveltimes provides the ability to image dips beyond 90 degrees (e. g. Wu, 2002). Finally, the eikonal equation solver is also useful for computing traveltimes and raypaths in seismic tomography applications.

Conclusions

The errors of the eikonal equation solver stem from both non-plane wave and variable velocity effects. The errors would be reduced when a small grid spacing is used. However using the small grid spacing would increase computation cost dramatically, especially for 3-D applications. The variable grid spacing method suggested in this paper can be used to make the eikonal equation solver accurate and robust without unnecessarily high computation cost.

References

Aldridge, D., and Oldenburg, D., 1993, Two-dimensional tomographic inversion with finite-difference traveltimes: Journal of Seismic Exploration, **2**, 257-274.

Hole, J., and Zelt, B., 1995, 3-D finite-difference reflection traveltimes: Geophys. J. Int., **121**, 427-434.

Podvin, P., and Lecomte, I., 1991, Finite difference computation of traveltimes in very contrasted velocity models: a massively parallel approach and its associated tools: Geophys. J. Int., **105**, 271-284.

Telford W., Geldart L., Sheriff R., and Keys D., 1976, Applied Geophysics: Cambridge University Press, New York.

Vidale, J., 1988, Finite-difference calculation of travel times: Bull. Seism. Soc. Am., **78**, 2062-2076.

Vidale, J., 1990, Finite-difference calculation of travel times in 3D: Geophysics, **55**, 521-526.

Wu, W.-J., 2002, Imaging dips beyond 90 degrees by a modified prestack Kirchhoff time migration: CSEG National Convention Technical Abstract.

Acknowledgement

I would like to thank Geo-X Systems Ltd. for permission to present this paper. I would also like to thank my colleagues, particularly Mike Perz, Fuchang Guo, Brent Sato, and Sandor Bezdan for their support.